Distribution of total mercury and methylated mercury species in Central Arctic Ocean water and ice

Marine Chemistry 242 (2022) 104105

Contents lists available at ScienceDirect

Marine Chemistry

journal homepage: www.elsevier.com/locate/marchem

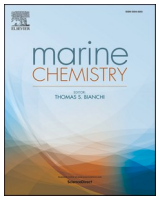

Distribution of total mercury and methylated mercury species in Central Arctic Ocean water and ice

Sofi Jonsson [a,b,c,*], Michelle G. Nerentorp Mastromonaco [d,e], Katarina Gårdfeldt [d], Robert P. Mason [b]

[a] Department of Environmental Science, Stockholm University, SE-106 91 Stockholm, Sweden
[b] Department of Marine Sciences, University of Connecticut, Groton CT06340, USA
[c] Center of Environmental and Sustainability, University of Gothenburg, SE-405 30 Gothenburg, Sweden
[d] Department of Chemistry and Chemical Engineering, Chalmers University of Technology, SE-412 96 Gothenburg, Sweden
[e] Swedish Environmental Research Institute, SE-411 33 Gothenburg, Sweden

A B S T R A C T

The central Arctic Ocean remains largely unexplored when it comes to the presence and cycling of mercury and its methylated forms including mono- and dimethylmercury (MMeHg and DMeHg, respectively). In this study, we quantified total Hg (Hg_T) and methylated Hg species in seawater, ice cores, snow, brine, and water from melt ponds collected during the SWEDARCTIC 2016 expedition to the Amerasian and Eurasian side of the Lomonosov Ridge. In the water column, concentrations of Hg_T, MMeHg and DMeHg ranged from 0.089 to 1.5 pM, <25 to 520 fM and from <1.6 to 160 fM, respectively. Hg_T was enriched in surface waters while MMeHg and DMeHg were low at the surface (i.e. in the polar mixed layer) and enriched at a water depth of around 200–400 m. A 1:2 ratio of DMeHg to MMeHg was observed in the water column suggesting a lower ratio in the central parts of the Arctic Ocean than what has previously been reported from other parts of the Arctic Ocean. At the ice stations, average Hg_T ranged from 0.97 ± 1.2 pM in the ice cores to 27 ± 17 pM in melt pond waters and average $MeHg_T$ (total MeHg) from 28 ± 15 fM in brine to 130 ± 18 fM in melt pond water. The Hg_T observed in melt ponds and brine was an order of magnitude greater than Hg_T observed in surface waters and Hg_T in the upper part of the ice-cores was ~4–8 times higher Hg_T in comparison to lower layers. Our study suggests that ice may act as a source of Hg_T to surface waters but not to be a likely source of the methylated Hg forms. Unlike elemental Hg, DMeHg did not enrich in surface waters covered by ice. Concentrations of DMeHg observed in the ice cores and other samples collected from the ice stations were low, suggesting ice to not act as a source of DMeHg to the atmosphere nor to surface waters.

1. Introduction

Mercury (Hg) is a toxic trace metal in marine systems that bioaccumulates as monomethylmercury (MMeHg) to concentrations of concern in the marine food webs. There are few local anthropogenic sources of Hg into the high Arctic region (Kirk et al., 2012), with only 2% of anthropogenic Hg inputs being from sources within the Arctic (AMAP, 2021). Even so, anthropogenically released Hg from lower latitudes is transported to the Arctic environment via long-range atmospheric transportation of elemental Hg (Hg^0). These anthropogenic sources of Hg are today primarily associated with artisanal gold mining and the burning of fossil fuel (coal) (Outridge et al., 2018).

Marine fish consumption is the main exposure route for MMeHg for most humans. In the Arctic, indigenous populations, who traditionally rely on a heavily marine based diet, are also being exposed to high MMeHg concentrations from the consumption of marine mammals (AMAP, 2011). Mercury cycling in the Arctic Ocean is therefore of particular concern. In the future, human exposure to the MMeHg accumulating in Arctic food webs could worsen as larger areas of the Arctic Ocean becomes attractive for commercial fishing as a consequence of increased access to the area with decreased sea ice coverage and the potential of fish stock migration into the area as water temperature rise. For the central Arctic Ocean, concerns are now being raised for a future "gold rush" of exploitation as international regulations are inadequate to protect the ecosystem and human health (Norris and Mckinley, 2016). Conversely, changing ice extent could also influence the air-sea exchange of Hg and the rate of formation and degradation of methylated Hg in the upper Arctic Ocean, and there is little consensus how the changes in sea ice extent will impact Hg dynamics due to the limited measurements of Hg speciation in waters of the open Arctic Ocean.

The two chemical forms of methylated Hg occurring in oceanic systems are MMeHg (CH_3HgX where X is Cl^{-1}, OH^{-1}, or organic thiols and other reduced sulfur ligands ($R\text{-}S^{-1}$)) and dimethylmercury ($(CH_3)_2Hg$,

* Corresponding author at: Department of Environmental Science, Stockholm University, SE-106 91 Stockholm, Sweden.
E-mail address: sofi.jonsson@aces.su.se (S. Jonsson).

https://doi.org/10.1016/j.marchem.2022.104105
Received 29 June 2021; Received in revised form 20 October 2021; Accepted 7 March 2022
Available online 12 March 2022

hereon referred to as DMeHg). While MMeHg is mostly present in the dissolved and particulate phase, DMeHg is present as a dissolved gas. MMeHg is the primary form of Hg that accumulates and magnifies in aquatic food webs and thus poses the greatest risk for human and wildlife health. For the Arctic Ocean, this MMeHg is hypothesized to primarily originate from land runoff, in situ production from bacterial transformation of inorganic Hg to MMeHg and from the potential decomposition of DMeHg (Heimbürger et al., 2015; Lehnherr et al., 2011; Soerensen et al., 2016). The role of DMeHg in the biogeochemical cycle of Hg and its bioaccumulative potential is largely unknown (AMAP, 2021). For the Arctic systems, several studies have suggested that the emission of DMeHg from the sea surface to the atmosphere, its subsequent decomposition in the atmosphere to MMeHg and its re-deposition could account for a substantial fraction of the MMeHg found in e.g. surface waters and snow sheets (Baya et al., 2015; St. Louis et al., 2005; St. Pierre et al., 2015). However, these studies have mostly focused on locations within the Canadian Arctic Archipelago (CAA) with little study being done in the open waters of the Arctic. Agather et al. (2019) did not find elevated concentrations of DMeHg in surface waters in the western parts of the central Arctic Ocean, suggesting that the emission of DMeHg to the atmosphere is less important than predicted based on the studies in the CAA.

The Arctic environment is currently undergoing dramatic changes, which is also affecting the biogeochemical cycle of Hg. Thawing permafrost is e.g. suggested to result in greater riverine discharge of Hg to the Arctic Ocean (Lim et al., 2019). Furthermore, the rapid loss of sea ice will have implications for the air-sea exchange of gaseous Hg species. Despite the urgency to understand in detail the biogeochemical cycle of Hg in the Arctic Ocean, many aspects of its cycle remain uncertain. To address this, a detailed examination of the speciation of Hg in the different Arctic Ocean compartments is needed. Observational data on Hg speciation from the central Arctic Ocean is however scarce (Agather et al., 2019; DiMento et al., 2019; Heimbürger et al., 2015; Schartup et al., 2020). Here, we report concentrations of total Hg (Hg_T), MMeHg and DMeHg along with ancillary parameters in the water column from stations sampled, covering four basins (Canada, Makarov, Amundsen and Nansen Basin) on the Amerasian and Eurasian side of the Lomonosov Ridge (Fig. 1). In addition, we measured the concentration of Hg_T and methylated Hg species in ice cores, snow, brine, melt and melt pond waters collected from ice stations to examine the potential inputs of methylated Hg from ice melt and from the atmosphere.

2. Material and methods

2.1. Sampling

Seawater, ice, brine, snow and water from melt ponds were sampled during the SWEDARCTIC 2016 expedition onboard the Swedish icebreaker Oden in the central Arctic Ocean (8th of August to 20th of September 2016). Seawater was sampled from fourteen stations from 82°N 141°W to 80°N 8°E covering the Canada, Makarov, Amundsen, Nansen and the East Greenland Rift Basins (Fig. 1). MMeHg and DMeHg was quantified at ten and Hg_T at eleven of these stations. In addition, $MeHg_T$ (total methylated Hg) was quantified at two of the stations where MeHg and DMeHg were not quantified. Further details on what analyte that was analyzed at which station is provided in Table S1. Contamination from conventional Niskin bottles, when used to sample sea water for mercury speciation, has previously been shown to be insignificant

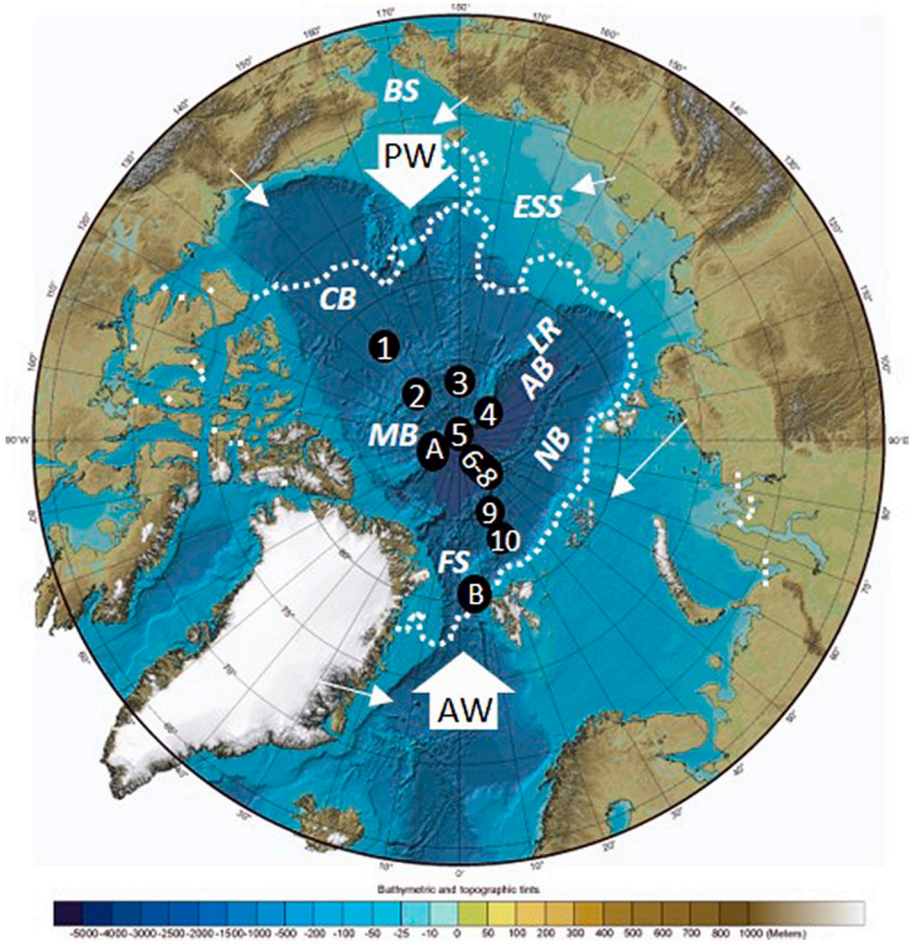

Fig. 1. The international bathymetric map of the Arctic Ocean (Jakobsson et al., 2012) with place names of major basins (Canada Basin, CB; Makarov Basin, MB; Amundsen Basin, AB; Nansen Basin, NB), Lomonosov Ridge (LR), Eastern Siberian Shelf (ESS) and main gateway straits (Bering Strait, BS; and Fram Strait, FS). Sampling locations where MMeHg and DMeHg were measured are shown as black dots with station number (1–10; Hg_T was quantified at station 1, 3–7 and 9). Location a and b, shows additional stations where seawater Hg_T and/or total methylated Hg (MMeHg+DMeHg) was quantified (A: Station 11 and 12, B: Station 13 and 14; Table S1). The dotted lines show the average sea ice extent for September 2016 (NSIDC, 2021). Inflow of Atlantic Ocean water (AW) and Pacific Ocean water (PW) into the Arctic Ocean are shown as bold white arrows. Main freshwater inputs from the watershed are shown as thin white arrows.

(Kotnik et al., 2007). Sampling of seawater was conducted using a rosette with Niskin bottles mounted on a metal frame together with a CTD system. Ice cores ($n = 7$), brine ($n = 10$), snow ($n = 3$), water from melt ponds ($n = 9$) and seawater from under the ice (n = 10) were collected from seventeen ice stations (Table S2, Fig. S1). Temperature depth profiles for five of the collected ice cores are presented in Fig. S2. $MeHg_T$ and Hg_T were quantified from a subset of these samples (Table S3 and S4). In addition, DMeHg was quantified in eight of the ice core samples, in water from two melt ponds and in two of the brine samples. Ice cores were sampled using a stainless-steel corer with cutting teeth and a diameter of 12 cm. The ice core was handled on clean surfaces and transported to the lab in sealed plastic bags. The surface of the cores were scraped with a Teflon scraper before being melted in gastight plastic bags as described by Nerentorp Mastromonaco et al. (2016). Brine was collected using a 0.5 L Teflon bottle attached to an aluminum bar from sack holes created during the sampling of ice cores. Under ice water was sampled in a similar way after extracting the entire ice core. Water from melt ponds were sampled using a Teflon bottle after breaking the overlying ice with a stainless-steel knife. All containers were cleaned 3 times with sampled water before being filled with the sample. "Clean hands-dirty hands" protocols were applied during sampling. MMeHg, $MeHg_T$ and Hg_T was subsampled in 250 and 150 mL glass amber bottles. Before sampling, all bottles were precleaned with 10% hydrochloric acid (1 week) for MMeHg and 0.5% BrCl (1 week) and 5% nitric acid (1 week) for Hg_T vials, before being rinsed with purified water ($\Omega > 18.2$ MΩ) and double bagged. DMeHg was sampled in 2 L acid washed Teflon bottles. The Teflon bottles were pre-cleaned before the expedition as described above for MMeHg analysis. During the expedition, the Teflon bottles were thoroughly rinsed with the sampled water prior to filling the bottles.

2.2. Chemical analysis

Samples collected for MMeHg and Hg_T were acidified with 0.4% trace metal clean H_2SO_4 (Fisher Chemical, trace metal grade) and shipped to the University of Connecticut for analysis (details of the analysis are provided in Supporting Information (SI)). The concentration of DMeHg was analyzed onboard the ship by purging 2 L of water for 30 min at a flow rate of 1 L min^{-1} with ultrapure Ar*(g)*. The purged gas was dried on a soda lime trap before trapping the analyte using a Carbotrap™ (Supelco) column. After drying the Carbotraps™ column for 10 min using ~100 mL min^{-1} Ar*(g)*, collected DMeHg was thermally desorbed, separated from other volatile Hg compounds collected by isothermal gas chromatography, pyrolytically decomposed to Hg^0 and detected using CVAFS (Tekran, model 2500). Given the high toxicity of DMeHg, other forms of Hg are commonly used for calibration purposes as all species are decomposed to Hg^0 before being detected (Black et al., 2009). In our case, we used a heated gold trap as the pyrolytical unit (i.e. to decompose Hg compounds after being separated in the GC column to Hg^0 prior to detection). Before desorbing each Carbotrap™ column, we trapped and desorbed 10 uL of gaseous Hg^0 vapor (from a Hg^0(l) source kept at 4 °C). The gold trap was then continually heated to work as the pyrolytical unit. The gold trap was heated using a nichrome wire coil (sufficient temperature to decompose the analytes to Hg^0 was assured by applying a current through the wire until a red glow was noted). The limit of detection (LOD) of 1.6 fM for DMeHg was calculated as 3 times the relative percent difference (RPD) of seawater duplicates with low concentrations of DMeHg (average concentration of the duplicates was 20 fM). The RPD for duplicate sample analyses was 6.7%.

Temperature, conductivity, depth and dissolved oxygen were measured using a CTD with attached oxygen sensors. Absolute salinity (Sa, g kg^{-1}), conservative temperature (Θ, °C) and potential density (ρ^{Θ}, kg m^{-3}) was then calculated using the TEOS-10 program (v3.05, http://www.teos-10.org) on MatLab. The inventory of freshwater content of the mixed layer (h_{fw}, m) was calculated between the surface and the 34 isohaline as described in (Rabe et al., 2011) (S_a of 35 kg m^{-3} was used as the reference salinity). For most of the Arctic Ocean, the 34 isohaline has shown to lie within the lower halocline and to be largely unaltered by the salinity of surface water, and thus be a suitable lower limit when calculating the freshwater content.

3. Results and discussion

3.1. Water mass characterization

The Arctic Ocean is an enclosed ocean that receives ~80% of its water from the North Atlantic Ocean via the Fram Strait and the Barents Sea (Jones, 2001). This Atlantic water (AW) freshens and cools as it enters the Eurasian basin and encounters the ice edge creating an embryonic halocline. The AW then undergoes several freezing and thawing cycles as it continues into the Amundsen basin and travels along the Lomonosov Ridge to then 'spill' into the Amerasian basin where it circulates into the Makarov- and Canada Basin. In addition to the AW, the Arctic Ocean receives Pacific Water (PW) through the Bering Strait (Fig. 1) and freshwater coming from rivers and precipitation. Together, river and atmospheric freshwater inputs form a surface polar mixed layer (PML) that enables the polar ice coverage to extend during fall and winter periods. The PW is, in comparison to the AW, fresher and enriches the halocline that separates the PML from the AW in the Amerasian Basin (Carmack et al., 2016). As most freshwater entering the ocean from rivers is directed towards the East Siberian Shelf before being pushed into the central parts of the ocean (in the same area as the inflow of PW), and as the AW enters the ocean from the opposite side via the Fram Strait (Fig. 1), a gradient is formed with a deeper PML and halocline in the Canadian Basin.

The depth of the polar mixed layer (PML) at the stations sampled was calculated based on an increased potential density (ρ^{Θ}, kg m^{-3}) of 0.01 kg m^{-3} relative to surface water (Toole et al., 2010), and ranged in depth from 7.5–35 m for the Central Arctic stations (Stations 1–12, Table S1). These PML depths are comparable to those reported from observations in the Canada Basin between 2004 and 2009 (averaging at around 20 m) (Toole et al., 2010). The depth of the halocline (from the PML boundary layer depth down to the 34 isohaline, Fig. 2) ranged from a total depth of 124 m (at a water depth of 26–150 m) in the Canada Basin to 13 and 17 m (water depth of 16–29 m and 15–32 m, respectively) for the two profiles sampled in the Nansen Basin (Table S1). The combined content of freshwater in the PML and halocline (height freshwater, h_{fw}, m) ranged from 15 m at Station 1 to 1.4 m at Station 10 (Table S1). The higher freshwater content, and deeper PML and halocline, observed in the Amerasian Basin (Station 1–3) in comparison to the stations on the Euroasian side of the Lomonosov ridge (Station 5–12) was expected given the geographical differences in the inflow of fresh water and AW into the central basin, as described above (Fig. 1). The conservative temperature (Θ, °C) maxima was found at depths of ~200–400 m at all stations and overall traces the warmer AW (Fig. 2, Fig. S4).

3.2. Total Hg

Bulk Hg_T in seawater ranged from 0.089 to 1.5 pM along the sampled transect and with depth (Table 1). These concentrations are in a similar range to the concentrations previously reported by Heimbürger et al. (2015) from the Eurasian basin (bulk Hg_T ranging from 0.45 to 7 pM) and by Agather et al. (2019) from the western parts of the central Arctic Ocean (filtered Hg_T ranging from 0.21 to 3.69 pM). Only a smaller fraction of Hg_T in Arctic seawater is particulate (Agather et al., 2019), explaining the similar ranges for bulk and filtrated Hg_T previously observed. At several stations, we observed an enrichment of Hg_T in surface waters (Figs. 3, S3 and S4). To test the distribution of the Hg species as a function of depth, the water column was divided into four sections; PML, halocline (the layer between the PML and the 34th isohaline), water below the halocline down to a water depth of 400 m and deep waters (water depth > 400 m). For Hg_T, we observed higher mean

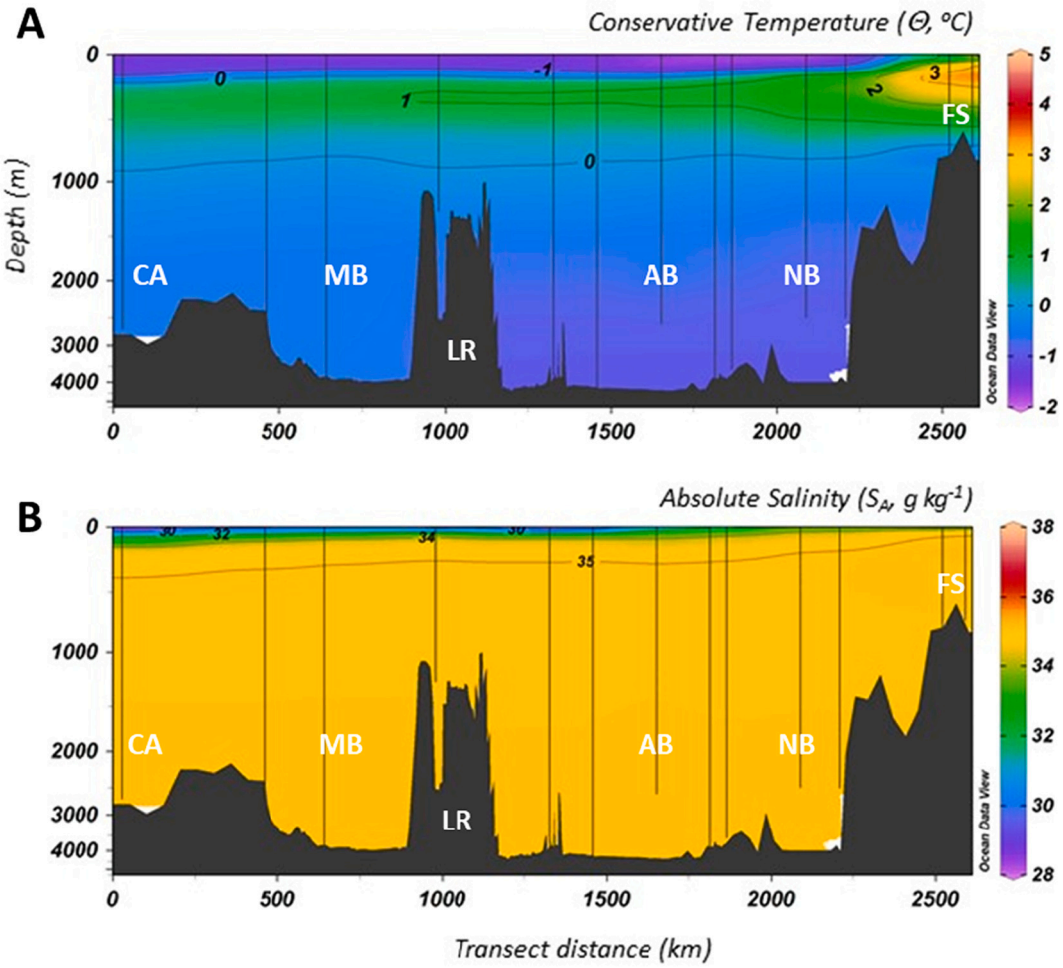

Fig. 2. A) conservative temperature (°C) and B) absolute salinity (g kg^{-1}) along the transect shown in Supplementary Fig. S3 during the SWEDARCTIC 2016 expedition in the central Arctic Ocean. Sampling stations and depths are shown as verticals lines and bathymetric features in gray. Letters indicate major basins (Canada Basin, CB; Makarov Basin, MB; Amundsen Basin, AB; Nansen Basin, NB), Lomonosov Ridge (LR) and Fram Strait (FS). Figures genenrated using Ocean Data view

Table 1
Range and average (±1 standard deviation) concentration of total Hg (Hg_T), monomethyl mercury (MMeHg), dimethylmercury (DMeHg) and total methylated Hg ($MeHg_T$) in the polar mixed layer (PML), halocline, below the halocline down to 400 m (halocline→400 m) and deep waters (>400 m) and for all the data.

	HgT (pM)[1]		MMeHg (fM)		DMeHg (fM)		$MeHg_T$ (fM)[1]	
	Range	Mean ± 1SD	Range	Mean ± 1SD	Range	Mean ± 1SD	Range	Mean ± 1SD
PML	0.64–1.3	$0.95 \pm 0.24^{(n=9)}$	<25–75	$31 \pm 15^{(n=11)}$	<1.6–7.1	$2.3 \pm 1.7^{(n=18)}$	25–76	$35 \pm 17^{(n=9)}$
Halocline	0.39–1.5	$0.74 \pm 0.32^{(n=14)}$	<25–150	$64 \pm 51^{(n=8)}$	<1.6–58	$24 \pm 17^{(n=24)}$	25–200	$87 \pm 65^{(n=11)}$
Halocline→400 m	0.089–0.8	$0.49 \pm 0.21^{(n=20)}$	<25–210	$100 \pm 54^{(n=20)}$	<1.6–110	$46 \pm 35^{(n=36)}$	25–320	$160 \pm 89^{(n=25)}$
> 400 m	0.15–0.88	$0.39 \pm 0.16^{(n=34)}$	<25–520	$110 \pm 100^{(n=29)}$	<1.6–160	$37 \pm 37^{(n=47)}$	42–540	$160 \pm 100^{(n=36)}$
all data	0.15–1.5	$0.54 \pm 0.29^{(n=77)}$	<25–520	$88 \pm 78^{(n=68)}$	<1.6–160	$32 \pm 33^{(n=125)}$	25–540	$134 \pm 96^{(n=81)}$

[1] $MeHg_T$ was directly analyzed or calculated as the sum of MMeHg and DMeHg ($MeHg_T$ = MMeHg + DMeHg).

concentrations of Hg in the PML and the halocline compared to deeper waters ($p < 0.05$). Furthermore, a negative correlation was found between Hg_T and salinity ($R^2 = 0.52$, $p < 0.0001$). Enrichment of Hg_T in surface waters have also previously been observed in e.g. the western part of the central Arctic Ocean (Agather et al., 2019), at stations close to the marginal sea ice zone in the Eurasian basin (Heimbürger et al., 2015) and in the Beaufort Sea (Wang et al., 2012). The surface enrichment of Hg_T may be attributed to Hg deposited directly from the atmosphere in open water, Hg released from sea-ice and/or derived via riverine inputs (Agather et al., 2019; Heimbürger et al., 2015; Soerensen et al., 2016; Wang et al., 2012). We also observe high Hg_T in melt ponds located on the sea ice, in brine and in the upper most layer of ice cores extracted (Fig. 4). The Hg_T observed in melt ponds and brine was an order of magnitude greater than Hg_T observed in surface waters (Table 1), supporting that melting ice may have contributed to the enrichment of Hg_T in the PML and halocline. These vertical trends in ice, and the relative concentrations in ice, snow and meltwater are similar to those of DiMento et al. (2019) for the western Arctic Ocean, and Schartup et al. (2020) for a transect across the central Arctic ocean.

Along a transect covering the western part of the central Arctic Ocean higher concentrations of Hg_T were noted in the transpolar drift (TPD) water mass compared to surface waters from ice-covered stations outside the TPD (Agather et al., 2019). We have no data available to evaluate the geographical extent of the TPD at the time of our sampling

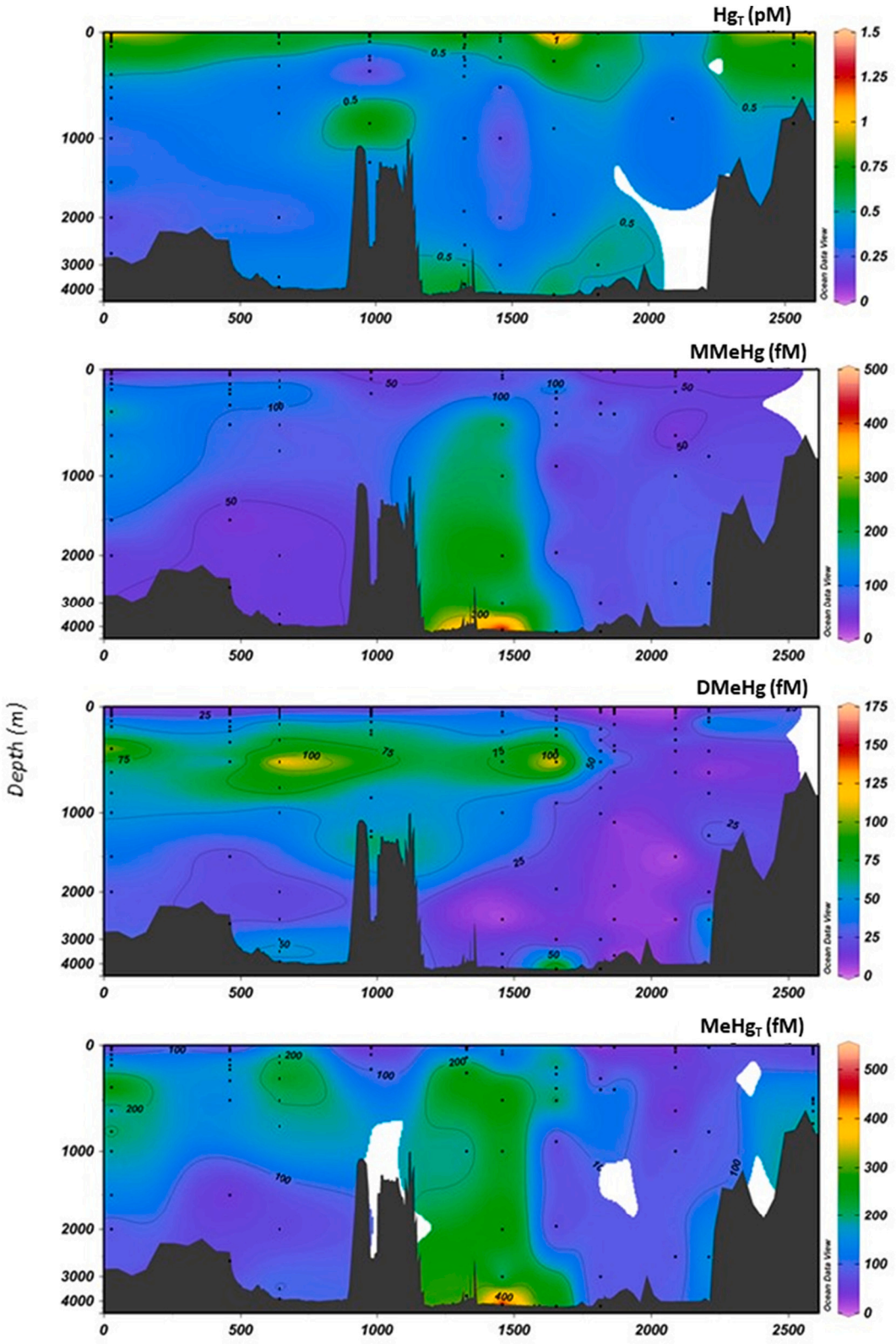

Fig. 3. Distribution of (a) Hg_T (pM), (b) total methylated Hg ($MeHg_T$, fM), (c) monomethylmercury (MMeHg, fM) and (d) dimethylmercury (DMeHg, fM) along the transect shown in supplementary Fig. S3 during the SWEDARCTIC 2016 expedition in the central Arctic Ocean. Sampling points are shown as black dots and bathymetric features in gray. Figures genenrated using Ocean Data view.

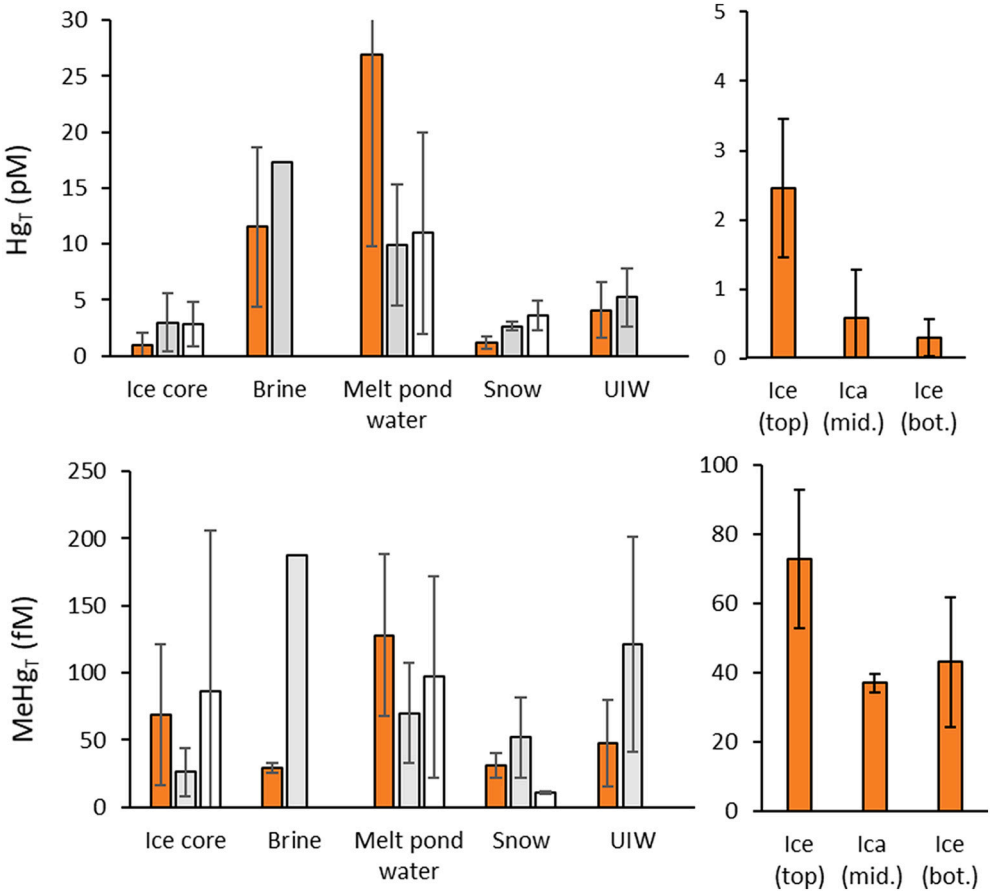

Fig. 4. Average (±1 SD) concentrations of Hg_T (top) and $MeHg_T$ (bottom) quantified from central Arctic Ocean ice cores, brine, melt pond water, snow and under-ice water (UIW) in this study (orange 1st bar), by Schartup et al., (2020) (light gray 2nd bar) and DiMento et al., (2019) (white 3rd bar). Right figure shows the concentrations of Hg_T and $MeHg_T$ in the top, middle (mid.) and bottom (bot.) section of the ice cores.

campaign. If assuming a similar lateral extent of the TPD as observed at the same time of the year in 2015 (TPD defined as the top 50 m from 84°N in the Canada Basin to 87°N in the Eurasian Basin (Charette et al., 2020)) we do, however, find similar Hg_T in the TPD and in the top 50 m at stations in the central Arctic Ocean outside the TPD ($p > 0.05$). Among four stations from the Eurasian basin, Heimbürger et al. (2015) noted the highest surface Hg_T close to the Laptev Sea, but low Hg_T at 90°N. Riverine inputs from the Lena River (the river with the highest annual load of Hg of the Arctic Rivers (Zolkos et al., 2020)) was suggested to explain high Hg_T close to the Laptev Sea, and algae bloom driven particle scavenging (as the water is moving north) to explain the low Hg_T at 90°N. In contrast to (Heimbürger et al., 2015), we note higher Hg_T in surface waters at 90°N (Station 5). It should however be noted that open leads were present also at 90°N at the time of sampling (satellite images also suggest an ice coverage around the north pole of ~80–90% in August when the station was sampled, Fig. S5). Atmospheric sources and melting sea ice could, thus, have contributed to the surface concentrations of Hg_T at 90°N in our study.

The distribution of Hg_T in ice, brine, snow and melt ponds have been previously studied in both Arctic and Antarctic ice-sheets (Beattie et al., 2014; Chaulk et al., 2011; DiMento et al., 2019; Nerentorp Mastromonaco et al., 2016; Schartup et al., 2020). These earlier studies have shown elevated Hg_T in the top-layer of both first-year and multiyear ice, and high Hg_T in brine and melt ponds (Beattie et al., 2014; Chaulk et al., 2011; DiMento et al., 2019; Nerentorp Mastromonaco et al., 2016; Schartup et al., 2020). In a similar way, we observed ~4–8 times higher Hg_T in the upper part of the ice-cores in comparison to lower layers (Fig. 4). Particles from e.g. sediments, aerosol sources and snow are known to accumulate in the surface layers of ice (Reimnitz et al., 1993; Tucker et al., 1999). These particles may also explain the phenomena of higher Hg_T at the surface of the ice (Beattie et al., 2014). In brine, Hg may be enriched as it is expelled from the ice during the freezing process. We also observe an order of magnitude higher Hg_T in brine and sea-ice in comparison to sub-surface ice layers and the sea-water (Table 1, Fig. 4). Observed Hg_T in sea-ice and brine are also close to the ranges of Hg_T reported in brine from Antarctic and Arctic ice-sheets (Antarctica: 64 ± 70 pM (Nerentorp Mastromonaco et al., 2016); 15 ± 5 pM (Cossa et al., 2011); Arctic: 13–360 pM (Chaulk et al., 2011)).

3.3. *MMeHg, DMeHg and $MeHg_T$*

The concentrations of MMeHg and DMeHg in the sea water ranged from <25 to 520 fM (average: 88 ± 96 fM) and from <1.6 to 160 fM (average: 32 ± 33 fM), respectively. For samples where $MeHg_T$ was determined (either by directly analyzing $MeHg_T$ or calculated from MMeHg and DMeHg, $n = 81$) the concentration of $MeHg_T$ ranged from <25 to 540 fM, (average $MeHg_T$ of 140 ± 96 fM). Only two studies have previously reported seawater MeHg in the central Arctic Ocean; Heimbürger et al. (2015) reporting $MeHg_T$ ranging up to 365 fM from stations in the Eurasian basin and Agather et al. (2019) reporting MMeHg and DMeHg ranging from <20 to 360 and < 12 to 230 fM, respectively, for the western Arctic Ocean. Our data on MMeHg, DMeHg and $MeHg_T$ agree well with these earlier reported ranges. From stations where we have both $MeHg_T$ and Hg_T, the fraction of Hg occurring as methylated Hg (%$MeHg_T$) ranged from 3.2 ± 0.81% ($n = 5$) in the PML to 18 ± 16% (n = 8) in the halocline and 53 ± 30% ($n = 22$) in deep waters. We note that some caution is warranted when interpreting the ratios of different Hg forms at these low concentrations as the analytical approaches

applied (in particular for Hg_T and MeHg as presented in the SI) may suffer from matrix interferences. The high $\%MeHg_T$ noted in deep water remained (average $\%MeHg_T$ of 41 ± 21%, $n = 17$) even after removing the data from the station with notably high MMeHg in deeper waters (Fig. 3). Agather et al. (2019) report average $\%MeHg_T$ of 12 ± 6% in the PML, 12 ± 9% in the halocline and 18 ± 17% in deep waters. Although the $\%MeHg_T$ we observe is similar to the $\%MeHg_T$ previously reported from the central Arctic Ocean, our data suggest a stronger gradient of $\%MeHg_T$ than what has previously been shown ($\%MeHg_T$ in PML and halocline < $\%MeHg_T$ below the halocline, $p < 0.05$).

At most stations, MMeHg was low in the PML and peaked at a water depth of around 200–400 m (MMeHg in PML < MMeHg below PML, $p < 0.05$, Fig. 3 and S3). At Station 5 in the Amundsen basin, high MMeHg was also observed in deep water (Fig. 3). Such high MMeHg was however not observed at the other stations. Although earlier studies have noted enrichments of MMeHg close to the sediments (Agather et al., 2019), this is unlikely to explain the high MMeHg observed in the deep waters collected hundreds or thousands of meters above the sediments. We also note that no enrichment in Hg_T or DMeHg was observed in the deep water collected from station 5.

Based on observations of high MMeHg in the oxygen minimum zone, in situ production of MMeHg has been coupled to the re-mineralizing of autotrophically formed carbon (Lehnherr et al., 2011; Wang et al., 2012). In other environments, such as inland waters and coastal sediments and waters, microorganisms carrying the Hg methylation genes (*hgcAB*) drives the production of MMeHg (Parks et al., 2013; Podar et al., 2015). It is unclear which processes dominate MMeHg production in the marine systems, as these genes are associated with anaerobic microorganisms and not typically found in marine systems or the Arctic Ocean (Bowman et al., 2019). Although their ability to methylate Hg has not been confirmed, the *Nitrospina* genus, has been put forth as a putative Hg methylator in Arctic Ocean waters (Bowman et al., 2019), as well as in other marine systems (Villar et al., 2019) and in Antarctic sea ice (Gionfriddo et al., 2016). A unique feature of the vertical profile of MMeHg in the Arctic Ocean, in comparison to other systems, is that the peak of MMeHg appears at a shallower depth (a few hundred meters in comparison to at ~1000 m in the Pacific and the Atlantic Ocean) (Agather et al., 2019; Heimbürger et al., 2015). Also in our study, we observe higher MMeHg in the top 400–500 m. The shallow maxima of MMeHg have been suggested to be an important factor explaining high Hg levels in Arctic biota, as the maxima is closer to the zone with a higher density of phytoplankton, which is an important part of MMeHg bioaccumulation into the base of the marine food web (Heimbürger et al., 2015; Wang et al., 2018).

At the ice stations, average $MeHg_T$ ranged from 28 ± 15 fM ($n = 8$) in brine to 130 ± 18 fM ($n = 6$) in melt pond water (Fig. 4; $MeHg_T$ in melt ponds water > $MeHg_T$ in ice, brine and under ice water, $p < 0.05$; $MeHg_T$ in brine < $MeHg_T$ in ice, $p < 0.05$). Higher $MeHg_T$ was observed in the top (73 ± 21 fM, $n = 4$) compared to the bottom (32 ± 21 fM, $n = 4$) of the ice cores (Fig. 4). The concentration of $MeHg_T$ observed was in the same range as $MeHg_T$ previously reported from the central Arctic Ocean (DiMento et al., 2019; Schartup et al., 2020). As for the water column, MMeHg in sea ice is suggested to be biologically produced in situ (Beattie et al., 2014; Cossa et al., 2011; Gionfriddo et al., 2016; Schartup et al., 2020). This inference has been supported by higher $MeHg_T$ in layers with high primary production (Beattie et al., 2014; Cossa et al., 2011; Gionfriddo et al., 2016), higher $MeHg_T$ content in the sea ice than in precipitation (DiMento et al., 2019; Gionfriddo et al., 2020), and the identification of putative Hg methylators in Antarctic sea ice (Gionfriddo et al., 2020). Although we do not have such data supporting the role of in situ methylation in the ice collected for this study, we note high $MeHg_T$ (~200 fM) in two ice samples collected in layers where algae were visually seen. While we find enriched concentrations of Hg_T in the brine in comparison to the ice, $MeHg_T$ did not differ between the two ($p > 0.05$), suggesting different processes to control the distribution of the two Hg forms (Hg_T mainly consisting of inorganic Hg species) between the ice and brine. The concentrations of $MeHg_T$ observed in ice, brine, snow (Fig. 4) are comparable to the concentrations of $MeHg_T$ observed in the PML (Table 1) and the concentrations of $MeHg_T$ in melt pond water comparable the average $MeHg_T$ found blow the PML. Although production of MMeHg within the ice may contribute to the pool of Hg accumulated in the marine food web, it is likely not the primary source given the similar concentrations of MMeHg in the water below and the larger volume of water masses with elevated MMeHg in comparison to the volume of sea ice.

As also observed elsewhere, the depth profile of DMeHg in the water column closely resembled that of MMeHg (Agather et al., 2019; Bowman et al., 2015). High DMeHg was, however, not observed at Station 5 where notably high concentrations of MMeHg were observed in the deep waters. In the PML, DMeHg was often below the detection limit and average DMeHg was lower in the PML than in the water masses below ($p < 0.05$). The DMeHg in the halocline was also lower than the DMeHg in the water mass below the halocline and down to 400 m ($p < 0.05$). Previous studies from the Arctic Ocean have reported a near 1:1 ratio of DMeHg to MMeHg from the Canadian Arctic Archipelago (Kirk et al., 2008) and a 2:1 ratio of DMeHg to MMeHg from the Fram Strait and the Barrens Sea Opening (Petrova et al., 2020). In contrast, a 1:2 ratio of DMeHg to MMeHg was observed both in our study and by Agather et al. (2019), suggesting lower DMeHg to MMeHg ratios in the central parts of the Arctic Ocean. What controls the DMeHg to MMeHg ratio in marine waters is currently unknown.

When biotic methylation of Hg was first shown in 1969, both production of MMeHg and DMeHg was observed (Jensen and Jernelov, 1969). Whereas the genes encoding for the proteins responsible for the transformation of inorganic Hg to MMeHg have been identified (Parks et al., 2013) the pathways for the formation of DMeHg still remains unidentified. Suggested pathways include the reaction of MMeHg with organic and inorganic reduced sulfide surfaces (Jonsson et al., 2016) and dissolved sulfide (Baldi et al., 1993). Existing data from incubation experiments of CAA waters suggests DMeHg formation rates from MMeHg ranging up to 0.16% d^{-1} and direct DMeHg formation rates from inorganic Hg that are one to two orders of magnitude lower (Lehnherr et al., 2011). At our stations, we observed typical DMeHg maxima at a water depth of 200–400 m (Fig. 4), possibly corresponding to a zone of higher remineralization but this also corresponds to the warmer AW. The mean residence time of the halocline created by AW and PW is ~10 yr, and the deeper Atlantic layers (200–300 m down to 900 m) have a residence time of ~25–30 yr (Macdonald et al., 2005). If assuming a concentration of DMeHg of ~170 fM for incoming AW (Petrova et al., 2020) and a degradation rate of 0.02% d^{-1} (Mason et al., 1995), ~80 fM and ~ 30 fM of DMeHg delivered with AW would remain after 10 and 25 years, respectively, suggesting in situ production would be necessary to explain the obtained concentrations in the corresponding water masses (Fig. 3). Likely, both input of DMeHg with incoming water and in situ formations contribute to the concentrations found in the sub-halocline waters in our study.

With the exception of 1 brine sample, where a concentration of 4.3 fM of DMeHg was measured, we could not detect DMeHg in sampled ice ($n = 8$), melt pond water ($n = 2$) and remaining brine samples ($n = 2$), suggesting reported concentrations of $MeHg_T$ in this study primarily consisted of MMeHg. This is in contrast to (Schartup et al., 2020) who reported 15 ± 15 to 48 ± 94 fM of DMeHg in three ice-cores from the Arctic Ocean (DMeHg corresponded to ~30% of $MeHg_T$). Why we find these differences are unclear but could reflect differences in ice thawing approaches and analysis protocols. However, we also found low DMeHg in ice cores from the Chukchi Sea, collected in May/June 2021 (Mason, pers. comm.). One difference between the studies is that while we directly determined the DMeHg, Schartup et al. (2020) quantified the DMeHg as the difference between $MeHg_T$ and MMeHg. The concentration of DMeHg observed in waters collected under the ice (<1.6 to 9.8 fM) was in the same range as the concentrations observed in the PML at a depth of a few meters (Table S3) using the rosette (< 1.6–7.1 fM). We

thus do not find any support for the ice as a source of DMeHg to Arctic Ocean waters, nor to the atmosphere as previously suggested (Schartup et al., 2020; Soerensen et al., 2016).

The low concentrations of DMeHg in the PML, and the gradual increase of the concentrations following the halocline to higher concentrations in subsurface waters suggest that the PML and the halocline play a role in the vertical distribution of DMeHg, and its fate. Enrichments of elemental Hg^0 under ice-covered surface waters, in comparison to open waters, was observed during the cruise (Nerentorp Mastromonaco et al., 2017) in line with earlier work from the Arctic Ocean (Andersson et al., 2008; DiMento et al., 2019). As the volatility of Hg^0 is similar to that of DMeHg (Henrys law constant, H′, for Hg^0 and DMeHg is respectively 0.153 and 0.145 at 0 °C (Talmi and Mesmer, 1975)), this suggests that the sea ice can act as a barrier for both volatile species. If gas evasion was the explanation for the low concentrations of DMeHg in the PML, it would be reasonable to assume that the PML would also be depleted in Hg^0 given the similar water solubility of the two gases, but it is not. Instead, the low concentrations of DMeHg in the PML observed in our study suggests that either the DMeHg is degraded within the PML and/or the formation rates of DMeHg are very low. Currently, the stability of DMeHg in Arctic waters is unknown. Prior studies on the stability of DMeHg in seawater are limited to Atlantic and Pacific seawater, lake water and waters from upwelling zones in Monterey Bay (Black et al., 2009; Mason et al., 1995; Mason, 1991; Mason and Sullivan, 1999). Early work by Mason et al. suggested net degradation rates of 0.02% d^{-1} based on observed concentrations of DMeHg in North Atlantic Deep Waters of different ages (Mason et al., 1995) and up to 90% d^{-1} (assuming 12 h:12 h light and dark cycles) for samples exposed to light and kept at 24–28 °C, and 16% d^{-1} for samples kept dark at 4 °C (Mason and Fitzgerald, 1993). Even though the authors note that the discrepancy between rates calculated from DMeHg concentrations of different water masses and the experimentally determined rates in the laboratory (questioning the potential of bottle effects), the DMeHg amendment experiments clearly demonstrate the potential for degradation of DMeHg in a variety of different natural waters. In a more recent study, (Black et al., 2009) could not detect any degradation of DMeHg in upwelled water from upwelling zones in Monterey Bay, but as no amendments were done (experiments based on ambient DMeHg) environmentally significant degradation rates could have occurred even if changes were below the LOD. Overall, these studies support the potential of substantial DMeHg degradation in the water column, and that DMeHg may act as a source of MMeHg throughout the water column.

3.4. Implication for the regional biogeochemical cycle of Hg and future research needs

The Arctic Ocean is a unique marine system, especially in terms of the biogeochemical cycling of Hg. Some of the aspects making it distinct from other marine systems includes the impact of sea-ice on the biogeochemical cycling of Hg as well as the large input of Hg from riverine systems (Schartup et al., 2020; Soerensen et al., 2010; Sonke et al., 2018; Zolkos et al., 2020), and the relatively large shelf area compared to other oceans. Indeed, coastal inputs (rivers, ice and glacier melt) are comparable to the inputs from the atmosphere (Dastoor et al., 2021) which is substantially different from other oceans which are dominated by atmospheric inputs. These aspects of the biogeochemical cycle of Hg will be impacted by the accelerated warming of the Arctic environment, and the reduction in the amount of multiyear ice (AMAP, 2021).

Eurasian rivers are key sources of Hg to the Arctic Ocean (Sonke et al., 2018). Before entering the Central Arctic Ocean, these water masses are transported over the world's largest shelf areas. To what extent inorganic and methylated Hg exported from these sources enters the Central Arctic Ocean is currently not known, but recent estimates suggest that deposition of Hg to the shelf sediment is high (Petrova et al., 2020). Although these riverine sources may have contributed to the Hg observed in the water collected from the TPD in our study, our data do not support higher Hg content in the TPD in comparison to surface water in other parts of the central Arctic Ocean. Although most of the Hg exported by these rivers are likely trapped in the shelf sediments (Petrova et al., 2020), few studies focusing on the biogeochemical cycle or the fate of Hg have focused on the important Eurasian shelf regions (Coquery et al., 1995; Kim et al., 2020; Van et al., 2022). Furthermore, information on the availability of Hg exported by these rivers is needed in order to link the quantities exported with the pool of Hg emitted to the atmosphere or accumulated in marine food webs (Zhang et al., 2015).

In the atmosphere, any evaded DMeHg can be degraded to MMeHg (Niki et al., 1983; Sommar et al., 1996). The re-deposition of the MMeHg formed from DMeHg emitted to the atmosphere from Arctic waters and ice have been previously suggested to be an important source of MMeHg to e.g. surface waters and snow (Baya et al., 2015; Schartup et al., 2020; Soerensen et al., 2016; St. Louis et al., 2005). Here, we observed lower DMeHg than what has been previously reported e.g. from the top 20 m within the CAA (17 ± 10–60 ± 70 fM (Baya et al., 2015; Kirk et al., 2008; Lehnherr et al., 2011; St. Louis et al., 2007)). Also, DMeHg was not enriched under the ice. The lack of DMeHg enrichment under the ice was also noted in the only previous study available where DMeHg was quantified in the central Arctic Ocean water column (Agather et al., 2019). Furthermore, the concentrations of DMeHg in collected ice, brine and melt pond water was low (in most cases below the detection limit). These observations suggest more moderate emissions of DMeHg than has been previously suggested based on data from the CAA by (Soerensen et al., 2016) (14 Mg a^{-1} for the entire region also including the central ocean that covers ~40% of the entire area). Furthermore, our study suggests that degradation of DMeHg in the water column may be a more important source of MMeHg in this system than the gaseous evasion of DMeHg and re-deposition of MMeHg after atmospheric demethylation. Although recent studies have explored the potential formation and degradation pathways of DMeHg (Jonsson et al., 2016; West et al., 2020) what drives the balance between the two methylated forms of Hg in the Arctic Ocean (and other marine systems) remains unknown. Lower MMeHg to DMeHg ratios were observed in the water of the central Arctic Ocean, both in our study and by (Agather et al., 2019), in comparison to the ratio observed in other parts of the Arctic Ocean and other marine systems (Petrova et al., 2020). Although our understanding of DMeHg cycling currently is too limited to explain these differences, observed differences offer insights into what may be the important drivers, and these processes require further investigation. Differences in productivity and light regimes could e.g. play a role in the conversion of Hg between the two methylated forms, and may account for differences observed because of the differences in the sampling season.

Based on ice concentration maps from November 2015 to October 2016 (NSIDC, 2021), examples provided in Fig. S5), we roughly estimated a 95% ice coverage in the central basin from November 2015 through May 2016 and a 50% ice coverage from April 2016 through October 2016. In fact, the ice coverage in summer 2016 was, at the time, the second lowest ever recorded since the minimum record in 2012 (Fig. S6). With the potential future human health risk associated with enhanced commercial fishing in the central Arctic Ocean (Norris and Mckinley, 2016), future studies are warranted to understand the impact that the expected future reduction of sea-ice may have on the cycling of methylated Hg in the central Arctic Ocean. A key component in any future work is to clearly understand the key formation and degradation processes of DMeHg in the different waters of the Arctic Ocean to fully understand the different sources of MMeHg to Arctic Ocean surface waters and biota.

Declaration of Competing Interest

None.

Acknowledgement

This work was funded by the Swedish Research Council (International Post Doc grand nr 637-2014-54 to S.J) and the Swedish Polar Research Secretariat as part of the research program SWEDARCTIC 2016. We would like to thank the crew on the icebreaker Oden, and the staff from the Swedish Polar Research Secretariat that facilitated the work onboard (Åsa Lindgren, Robert Holden, Lars Lehnert, Axel Meiton and Per Salo). S.J would also like to thank Katlin Bowman for sharing previous expedition experiences, Prentiss Balcom for valuable support during the planning as well as for providing technical expertise, and well as the other scientists participating on the cruise. The University of Connecticut and the National Science Foundation (OCE 1434998 & 1260416) is also acknowledged for their previous contribution to the analytical instrumentation used and the laboratory facilities.

Appendix A. Supplementary data

Supplementary data to this article can be found online at https://doi.org/10.1016/j.marchem.2022.104105.

References

Agather, A.M., Bowman, K.L., Lamborg, C.H., Hammerschmidt, C.R., 2019. Distribution of mercury species in the Western Arctic Ocean (U.S. GEOTRACES GN01). Mar. Chem. 216, 103686 https://doi.org/10.1016/j.marchem.2019.103686.

AMAP, 2011. AMAP Assessment 2011: Mercury in the Arctic. Oslo, Norway, Arctic Monitoring and Assessment Programme (AMAP).

AMAP, 2021. 2021 AMAP Mercury Assessment. Summary for Policy-makers, Oslo, Norway.

Andersson, M.E., Sommar, J., Gårdfeldt, K., Lindqvist, O., 2008. Enhanced concentrations of dissolved gaseous mercury in the surface waters of the Arctic Ocean. Mar. Chem. 110, 190–194. https://doi.org/10.1016/j.marchem.2008.04.002.

Baldi, F., Pepi, M., Filippelli, M., 1993. Methylmercury resistance in desulfovibrio desulfuricans strains in relation to methylmercury degradation. Appl. Environ. Microbiol. 59, 2479–2485.

Baya, P.A., Gosselin, M., Lehnherr, I., Louis, V.L.S., Hintelmann, H., 2015. Determination of monomethylmercury and dimethylmercury in the arctic marine boundary layer. Environ. Sci. Technol. 49, 223–232. https://doi.org/10.1021/es502601z.

Beattie, S.A., Armstrong, D., Chaulk, A., Comte, J., Gosselin, M., Wang, F., 2014. Total and methylated mercury in arctic multiyear sea ice. Environ. Sci. Technol. 48, 5575–5582. https://doi.org/10.1021/es5008033.

Black, F.J., Conaway, C.H., Flegal, A.R., 2009. Stability of dimethyl mercury in seawater and its conversion to monomethyl mercury. Environ. Sci. Technol. 43, 4056–4062. https://doi.org/10.1021/es9001218.

Bowman, K.L., Hammerschmidt, C.R., Lamborg, C.H., Swarr, G., 2015. Mercury in the North Atlantic Ocean: the U.S. GEOTRACES zonal and meridional sections. Deep. Res. Part II Top. Stud. Oceanogr. 116, 251–261. https://doi.org/10.1016/j.dsr2.2014.07.004.

Bowman, K.L., Collins, R.E., Agather, A.M., Lamborg, C.H., Hammerschmidt, C.R., Kaul, D., Dupont, C.L., Christensen, G.A., Elias, D.A., 2019. Distribution of mercury-cycling genes in the Arctic and equatorial Pacific oceans and their relationship to mercury speciation. Limnol. Oceanogr. lno.11310 https://doi.org/10.1002/lno.11310.

Carmack, E.C., Haine, T.W.N., Bacon, S., Bluhm, B.A., Lique, C., Melling, H., Polyakov, I. V., Straneo, F., Timmermans, M., Williams, W.J., 2016. Freshwater and its role in the Arctic marine system: sources, disposition, storage, export, and physical and biogeochemical consequences in the Arctic and global oceans. J. Geophys. Res. Biogeosci. 121, 675–717. https://doi.org/10.1002/2015JG003140. 10.1002/2015JG003140.Received.

Charette, M.A., Kipp, L.E., Jensen, L.T., Dabrowski, J.S., Whitmore, L.M., Fitzsimmons, J. N., Williford, T., Ulfsbo, A., Jones, E., Bundy, R.M., Vivancos, S.M., Pahnke, K., John, S.G., Xiang, Y., Hatta, M., Petrova, M.V., Heimbürger-Boavida, L.-E., Bauch, D., Newton, R., Pasqualini, A., Agather, A.M., Amon, R.M.W., Anderson, R.F., Andersson, P.S., Benner, R., Bowman, K.L., Edwards, R.L., Gdaniec, S., Gerringa, L.J. A., González, A.G., Granskog, M., Haley, B., Hammerschmidt, C.R., Hansell, D.A., Henderson, P.B., Kadko, D.C., Kaiser, K., Laan, P., Lam, P.J., Lamborg, C.H., Levier, M., Li, X., Margolin, A.R., Measures, C., Middag, R., Millero, F.J., Moore, W. S., Paffrath, R., Planquette, H., Rabe, B., Reader, H., Rember, R., Rijkenberg, M.J.A., Roy-Barman, M., Rutgers van der Loeff, M., Saito, M., Schauer, U., Schlosser, P., Sherrell, R.M., Shiller, A.M., Slagter, H., Sonke, J.E., Stedmon, C., Woosley, R.J., Valk, O., van Ooijen, J., Zhang, R., 2020. The transpolar drift as a source of riverine and shelf-derived trace elements to the Central Arctic Ocean. J. Geophys. Res. Ocean. 125 https://doi.org/10.1029/2019JC015920.

Chaulk, A., Stern, G.A., Armstrong, D., Barber, D.G., Wang, F., 2011. Mercury distribution and transport across the ocean-sea-ice-atmosphere interface in the arctic ocean. Environ. Sci. Technol. 45, 1866–1872. https://doi.org/10.1021/es103434c.

Coquery, M., Cossa, D., Martin, J.M., 1995. The distribution of dissolved and particulate mercury in three Siberian estuaries and adjacent Arctic coastal waters. Water Air Soil Pollut. 80, 653–664. https://doi.org/10.1007/BF01189718.

Cossa, D., Heimbürger, L.-E., Lannuzel, D., Rintoul, S.R., Butler, E.C.V., Bowie, A.R., Averty, B., Watson, R.J., Remenyi, T., 2011. Mercury in the Southern Ocean. Geochim. Cosmochim. Acta 75, 4037–4052. https://doi.org/10.1016/j.gca.2011.05.001.

Dastoor, A.H. Angot, Bieser, J., Christensen, J.H., Douglas, T.A., Heimbürger-Boavida, L.-E., Jiskra, M.J., Mason, R.P., McLagan, D.S., Obrist, D., Outridge, P.M., Petrova, M. V., Ryjkov, A., St Pierre, K.A., Schartup, K.A., Soerensen, A.L., Toyota, K., Travnikov, O., Wilson, S.J., Zdanowicz, C., 2021. Arctic Mercury Cycling. Submitt. to Nat. Rev, Earth Environ.

DiMento, B.P., Mason, R.P., Brooks, S., Moore, C., 2019. The impact of sea ice on the air-sea exchange of mercury in the Arctic Ocean. Deep. Res. Part I Oceanogr. Res. Pap. 144, 28–38. https://doi.org/10.1016/j.dsr.2018.12.001.

Gionfriddo, C.M., Tate, M.T., Wick, R.R., Schultz, M.B., Zemla, A., Thelen, M.P., Schofield, R., Krabbenhoft, D.P., Holt, K.E., Moreau, J.W., 2016. Microbial mercury methylation in Antarctic Sea ice. Nat. Microbiol. 1, 16127. https://doi.org/10.1038/nmicrobiol.2016.127.

Gionfriddo, C.M., Stott, M.B., Power, J.F., Ogorek, J.M., Krabbenhoft, D.P., Wick, R., Holt, K., Chen, L.X., Thomas, B.C., Banfield, J.F., Moreau, J.W., 2020. Genome-resolved metagenomics and detailed geochemical speciation analyses yield new insights into microbial mercury cycling in geothermal springs. Appl. Environ. Microbiol. 86 https://doi.org/10.1128/AEM.00176-20.

Heimbürger, L.-E., Sonke, J.E., Cossa, D., Point, D., Lagane, C., Laffont, L., Galfond, B.T., Nicolaus, M., Rabe, B., van der Loeff, M.R., 2015. Shallow methylmercury production in the marginal sea ice zone of the Central Arctic Ocean. Sci. Rep. 1–6 https://doi.org/10.1038/srep10318. 10.1038/srep10318.

Jakobsson, M., Mayer, L., Coakley, B., Dowdeswell, J.A., Forbes, S., Fridman, B., Hodnesdal, H., Noormets, R., Pedersen, R., Rebesco, M., Schenke, H.W., Zarayskaya, Y., Accettella, D., Armstrong, A., Anderson, R.M., Bienhoff, P., Camerlenghi, A., Church, I., Edwards, M., Gardner, J.V., Hall, J.K., Hell, B., Hestvik, O., Kristoffersen, Y., Marcussen, C., Mohammad, R., Mosher, D., Nghiem, S. V., Pedrosa, M.T., Travaglini, P.G., Weatherall, P., 2012. The international bathymetric chart of the Arctic Ocean (IBCAO) version 3.0. Geophys. Res. Lett. 39, 12609. https://doi.org/10.1029/2012GL052219.

Jensen, S., Jernelov, A., 1969. Biological methylation of mercury in aquatic organisms. Nature 223, 753–754.

Jones, E.P., 2001. Circulation in the Arctic Ocean. Polar Res. 20, 139–146.

Jonsson, S., Mazrui, N.M., Mason, R.P., 2016. Dimethylmercury formation mediated by inorganic and organic reduced sulfur surfaces. Sci. Rep. 6, 27958. https://doi.org/10.1038/srep27958. 10.1038/srep27958.

Kim, J., Soerensen, A.L., Kim, M.S., Eom, S., Rhee, T.S., Jin, Y.K., Han, S., 2020. Mass budget of methylmercury in the east Siberian Sea: the importance of sediment sources. Environ. Sci. Technol. 54, 9949–9957. https://doi.org/10.1021/acs.est.0c00154.

Kirk, J.L., St Louis, V., Hintelmann, H., Lehnherr, I., Else, B., Poissant, L., 2008. Methylated mercury species in marine waters of the Canadian high and sub Arctic. Environ. Sci. Technol. 42, 8367–8373.

Kirk, J.L., Lehnherr, I., Andersson, M., Braune, B.M., Chan, L., Dastoor, A.P., Durnford, D., Gleason, A.L., Loseto, L.L., Steffen, A., St Louis, V.L., 2012. Mercury in Arctic marine ecosystems: sources, pathways and exposure. Environ. Res. 119, 64–87. https://doi.org/10.1016/j.envres.2012.08.012.

Kotnik, J., Horvat, M., Tessier, E., Ogrinc, N., Monperrus, M., Amouroux, D., Fajon, V., Gibičar, D., Žižek, S., Sprovieri, F., Pirrone, N., 2007. Mercury speciation in surface and deep waters of the Mediterranean Sea. Mar. Chem. 107, 13–30. https://doi.org/10.1016/j.marchem.2007.02.012.

Lehnherr, I., St Louis, V.L., Hintelmann, H., Kirk, J.L., 2011. Methylation of inorganic mercury in polar marine waters. Nat. Geosci. 4, 298–302. DOI: 10.1038/NGEO1134 Methylation. doi:10.1038/ngeo1134.

Lim, A.G., Sonke, J.E., Krickov, I.V., Manasypov, R.M., Loiko, S.V., Pokrovsky, O.S., 2019. Enhanced particulate hg export at the permafrost boundary, western Siberia. Environ. Pollut. 254, 113083 https://doi.org/10.1016/j.envpol.2019.113083.

Macdonald, R.W., Harner, T., Fyfe, J., 2005. Recent climate change in the Arctic and its impact on contaminant pathways and interpretation of temporal trend data. Sci. Total Environ. 342, 5–86. https://doi.org/10.1016/j.scitotenv.2004.12.059. doi:10.1016/j.scitotenv.2004.12.059.

Mason, R.P., 1991. Chemistry of Mercury in the Equatorial Pacific Ocean. University of Connecticut.

Mason, R.P., Fitzgerald, W.F., 1993. The distribution and biogeochemical cycling of mercury in the equatorial Pacific Ocean. Deep-Sea Res. I Oceanogr. Res. Pap. 40, 1897–1924.

Mason, R.P., Sullivan, K.A., 1999. The distribution and speciation of mercury in the south and equatorial Atlantic. Deep. Res. Part II Top. Stud. Oceanogr. 46, 937–956. https://doi.org/10.1016/S0967-0645(99)00010-7.

Mason, R., Rolfhus, K., Fitzgerald, W., 1995. Methylated and elemental mercury cycling in surface and deep ocean waters of the North Atlantic. Water Air Soil Pollut. 80, 665–677.

Nerentorp Mastromonaco, M.G., Gårdfeldt, K., Langer, S., Dommergue, A., 2016. Seasonal study of mercury species in the Antarctic Sea ice environment. Environ. Sci. Technol. 50, 12705–12712. https://doi.org/10.1021/acs.est.6b02700.

Nerentorp Mastromonaco, M., Jonsson, S., Gårdfeldt, K., 2017. Air-sea exchange of elemental mercury over the open Arctic Sea. In: 13th International Conference on Mercury as a Global Pollutant.

Niki, H., Maker, P.S., Savage, C.M., Breitenbach, L.P., 1983. A fourier transform infrared study of the kinetics and mechanism for the reaction of atomic chlorine with

dimethylmercury. J. Phys. Chem. 87, 3722–3724. https://doi.org/10.1021/j100242a029.
Norris, A.J., Mckinley, P., 2016. The Central Arctic Ocean-preventing another tragedy of the commons. Polar Rec. (Gr. Brit). 1–9 https://doi.org/10.1017/S003224741600067X.
NSIDC, 2021. National Snow and Ice Data Centre [WWW Document]. URL. https://nsidc.org.
Outridge, P.M., Mason, R.P., Wang, F., Guerrero, S., Heimbürger-Boavida, L.-E., 2018. Updated global and oceanic mercury budgets for the United Nations global mercury assessment 2018. Environ. Sci. Technol. https://doi.org/10.1021/acs.est.8b01246.
Parks, J.M., Johs, A., Podar, M., Bridou, R., Hurt, R.A., Smith, S.D., Tomanicek, S.J., Qian, Y., Brown, S.D., Brandt, C.C., Palumbo, A.V., Smith, J.C., Wall, J.D., Elias, D. A., Liang, L., 2013. The genetic basis for bacterial mercury methylation. Science (80-.). 339, 1332–1335. https://doi.org/10.1126/science.1230667.
Petrova, M.V., Krisch, S., Lodeiro, P., Valk, O., Dufour, A., Rijkenberg, M.J.A., Achterberg, E.P., Rabe, B., Rutgers van der Loeff, M., Hamelin, B., Sonke, J.E., Garnier, C., Heimbürger-Boavida, L.-E., 2020. Mercury species export from the Arctic to the Atlantic Ocean. Mar. Chem. 225, 103855 https://doi.org/10.1016/j.marchem.2020.103855.
Podar, M., Gilmour, C.C., Brandt, C.C., Soren, A., Brown, S.D., Crable, B.R., Palumbo, A. V., Somenahally, A.C., Elias, D.A., 2015. Global Prevalence and Distribution of Genes and Microorganisms Involved in Mercury Methylation, pp. 1–13. https://doi.org/10.1126/sciadv.1500675.
Rabe, B., Karcher, M., Schauer, U., Toole, J.M., Krishfield, R.A., Pisarev, S., Kauker, F., Gerdes, R., Kikuchi, T., 2011. An assessment of Arctic Ocean freshwater content changes from the 1990s to the 2006–2008 period. Deep. Res. I 58, 173–185. https://doi.org/10.1016/j.dsr.2010.12.002.
Reimnitz, E., Barnes, P.W., Weber, W.S., 1993. Particulate matter in pack ice of the Beaufort gyre. J. Glaciol. 39, 186–198. https://doi.org/10.3189/s0022143000015823.
Schartup, A.T., Soerensen, A.L., Heimbürger-Boavida, L.-E., 2020. Influence of the Arctic Sea-ice regime shift on sea-ice methylated mercury trends. Environ. Sci. Technol. Lett 7, 708–713. https://doi.org/10.1021/acs.estlett.0c00465.
Soerensen, A.L., Sunderland, E.M., Holmes, C.D., Jacob, D.J., Yantosca, R.M., Skov, H., Christensen, J.H., Strode, S.A., Mason, R.P., 2010. An improved global model for air-sea exchange of mercury: high concentrations over the North Atlantic. Environ. Sci. Technol. 44, 8574–8580. https://doi.org/10.1021/es102032g.
Soerensen, A.L., Jacob, D.J., Schartup, A.T., Fisher, J.A., Lehnherr, I., St. Louis, V.L., Heimbürger, L.-E., Sonke, J.E., Krabbenhoft, D.P., Sunderland, E.M., 2016. A mass budget for mercury and methylmercury in the Arctic Ocean. Glob. Biogeochem. Cycles 30, 560–575. https://doi.org/10.1002/2015GB005280. 10.1002/2015GB005280.Received.
Sommar, J., Hallquist, M., Ljungström, E., 1996. Rate of Reaction between the Nitrate Radical and Dimethyl Mercury in the Gas Phase. Chem. Phys, Lett, p. 257.
Sonke, J.E., Teisserenc, R., Heimbürger-Boavida, L.-E., Petrova, M.V., Marusczak, N., Le Dantec, T., Chupakov, A.V., Li, C., Thackray, C.P., Sunderland, E.M., Tananaev, N., Pokrovsky, O.S., 2018. Eurasian river spring flood observations support net Arctic Ocean mercury export to the atmosphere and Atlantic Ocean. Proc. Natl. Acad. Sci. U. S. A. 115, E11586–E11594. https://doi.org/10.1073/pnas.1811957115.
St. Louis, V.L., Sharp, M.J., Steffen, A., May, A., Barker, J., Kirk, J.L., Kelly, D.D., Arnott, S.E., Keatley, B., Smol, J.P., 2005. Some sources and sinks of monomethyl and inorganic mercury on Ellesmere Island in the Canadian high Arctic. Environ. Sci. Technol. 39, 2686–2701. https://doi.org/10.1021/es049326o.
St. Louis, V.L., Hintelmann, H., Graydon, J.A., Kirk, J.L., Barker, J., Dimock, B., Sharp, M. J., Lehnherr, I., 2007. Methylated mercury species in Canadian high arctic marine surface waters and snowpacks. Environ. Sci. Technol. 41, 6433–6441. https://doi.org/10.1021/es070692s.
St. Pierre, K.A., St. Louis, V.L., Kirk, J.L., Lehnherr, I., Wang, S., La Farge, C., 2015. Importance of open marine waters to the enrichment of total mercury and monomethylmercury in lichens in the Canadian high arctic. Environ. Sci. Technol. 49, 5930–5938. https://doi.org/10.1021/acs.est.5b00347.
Talmi, Y., Mesmer, R.E., 1975. Studies on vaporization and halogen decomposition of methylmercury compounds using gc with a microwave detector. Water Res. 547–552.
Toole, J.M., Timmermans, M.L., Perovich, D.K., Krishfield, R.A., Proshutinsky, A., Richter-Menge, J.A., 2010. Influences of the ocean surface mixed layer and thermohaline stratification on Arctic Sea ice in the Central Canada Basin. J. Geophys. Res. 115, C10018. https://doi.org/10.1029/2009JC005660.
Tucker, W.B.I., Gow, A.J., Meese, D.A., Bosworth, H.W., Reimnitz, E., 1999. Physical characteristics of summer sea ice across the Arctic Ocean. J. Geophys. Res. C Ocean. 104, 1489–1504.
Van, L-N, Wild, B, Gustafsson, Ö, Semiletov, I., Dudarev, O., Jonsson, S., 2022. Spatial patterns and distributional controls of total and methylated mercury off the Lena River in the Laptev Sea sediments. Marine Chem. 238, 104052. https://www.sciencedirect.com/science/article/pii/S0304420321001377.
Villar, E., Cabrol, L., Heimbürger-Boavida, L.-E., 2019. Widespread microbial mercury methylation genes in the global ocean. bioRxiv 648329. https://doi.org/10.1101/648329.
Wang, F., Macdonald, R., Armstrong, D., Stern, G., 2012. Total and methylated mercury in the Beauford Sea: the role of local and recent organic remineralization. Environ. Sci. Technol. 46, 11821–11828.
Wang, K., Munson, K.M., Beaupré-Laperrière, A., Mucci, A., Macdonald, R.W., Wang, F., 2018. Subsurface seawater methylmercury maximum explains biotic mercury concentrations in the Canadian Arctic. Sci. Rep. 8, 14465. https://doi.org/10.1038/s41598-018-32760-0.
West, J., Graham, A.M., Liem-Nguyen, V., Jonsson, S., 2020. Dimethylmercury degradation by dissolved sulfide and Mackinawite. Environ. Sci. Technol. 54, 13731–13738. https://doi.org/10.1021/acs.est.0c04134.
Zhang, Y., Jacob, D.J., Dutkiewicz, S., Amos, H.M., Long, M.S., Sunderland, E.M., 2015. Biogeochemical drivers of the fate of riverine mercury discharged to the global and Arctic oceans. Glob. Biogeochem. Cycles 29, 854–864. https://doi.org/10.1002/2015GB005124.
Zolkos, S., Krabbenhoft, D.P., Suslova, A., Tank, S.E., McClelland, J.W., Spencer, R.G.M., Shiklomanov, A., Zhulidov, A.V., Gurtovaya, T., Zimov, N., Zimov, S., Mutter, E.A., Kutny, L., Amos, E., Holmes, R.M., 2020. Mercury export from Arctic great Rivers. Environ. Sci. Technol. 54, 4140–4148. https://doi.org/10.1021/acs.est.9b07145.
Schlitzer, Reiner, Ocean Data View, https://odv.awi.de, 2022.